Article:
Zhang, S. orcid.org/0000-0002-7905-927X and Lang, Z.-Q. (2020) SCADA-data-based wind turbine fault detection : a dynamic model sensor method. Control Engineering Practice, 102. 104546. ISSN 0967-0661

https://doi.org/10.1016/j.conengprac.2020.104546

SCADA-data-based wind turbine fault detection: a dynamic model sensor method

Sikai Zhang[a], Zi-Qiang Lang[a,*]

[a]*Department of Automatic Control and Systems Engineering, The University of Sheffield, Sheffield, United Kingdom*

Abstract

Fault detection based on data from the supervisory control and data acquisition (SCADA) system, which has been installed in most MW-scale wind turbines, has brought significant benefits for wind farm operators. However, the changes in the features of hardware sensor measurements, which are used in current SCADA systems, often cannot provide reliable early alarms. In order to resolve this problem, in this paper, a novel dynamic model sensor method is proposed for the SCADA data based wind turbine fault detection. A dynamic model representing the relationship between the generator temperature, wind speed, and ambient temperature is derived following the first principles and used as the basic structure of the model sensor. When the model sensor is applied for fault detection, its parameters are updated regularly using the generator temperature, wind speed, and ambient temperature data from the SCADA system. Then, from the updated model, the fault sensitive features of wind turbine system are extracted via performing system frequency analysis and used for the turbine fault detection. This novel model sensor method is applied to the SCADA data of a wind farm of 3 wind turbines currently operating in Spain. The results show that the proposed method can not only detect the turbine generator fault but also reveal the trend of ageing with the wind turbine generator, demonstrating its capability of failure prognosis for wind turbine system and components.

Keywords: SCADA systems, fault detection, frequency response, NOFRFs, nonlinear systems, wind energy

1. Introduction

The wind power generation, as a mainstream option for sustainable energy, requires timely fault detection for reducing the cost of operation and maintenance (O&M) (Lu et al., 2009). However, many advanced fault detection approaches are difficult to be implemented in practice due to the need of additional equipment that may incur considerable costs (Sun et al., 2016). Therefore, fault detection based on data from supervisory control and data acquisition (SCADA) systems, which have been installed in most MW-scale wind turbines, has attracted extensive research attention (Gray and Watson, 2010; Feng et al., 2011; Yang et al., 2013; Schlechtingen et al., 2013; Schlechtingen and Santos, 2014; Leahy et al., 2016; Hu et al., 2016; Wang et al., 2017; Pandit and Infield, 2018; Zhang et al., 2020).

From the raw data of traditional hardware sensor measurements, simple signal processing techniques are often used to detect wind turbine faults by checking whether the values of some measurements have exceeded a threshold (Qiu et al., 2012), or whether the trend of the measurements with a particular wind turbine is significantly different from that with the neighboring wind turbines (Wilkinson et al., 2014). However, hardware sensors in SCADA systems cannot directly measure some physical variables such as bending moments and drive-train torques, which are important indicators for wind turbine failures. Consequently, the techniques of soft sensors have been applied to estimate the immeasurable information from the measurable physical variables (Barahona et al., 2017; Alvarez and Ribaric, 2018). A soft sensor is basically a predictive model that is used to infer critical but difficult-to-measure physical variables (Kadlec et al., 2009; Kadlec and Gabrys, 2011). For example, the wind turbine shaft torque is vital for bearing fatigue life prognostic but difficult to measure directly; thus, soft sensors were used to estimate shaft torque from the measured generator power output and shaft rotational speed (Gray and Watson, 2010; Alvarez and Ribaric, 2018). Principle component analysis (PCA) techniques can also be used as soft sensors to estimate the damage sensitive latent variables. Jia et al. (2016) used the standard deviation of the secondary principle component (PC2) derived from measurable SCADA parameters as the indicator of wind turbine failures.

However, many damage sensitive features cannot be revealed by individual measurements but are embedded in the relationship between these measurements. For example, the power curve which shows the relationship between the wind speed and wind turbine power output has been used for wind turbine fault detections (Uluyol et al., 2011; Lydia et al., 2014; Carrillo et al., 2013; Shokrzadeh et al., 2014). Hereafter, we will refer to such a relationship as the model sensor where the features of the relationship between measurements rather than the measurements themselves are used to evaluate the health conditions of underlying systems.

An illustration of hardware sensors, soft sensors, and model sensors is shown in Fig. 1. The system in Fig. 1 can be a whole

*Corresponding author

Email addresses: szhang42@sheffield.ac.uk (Sikai Zhang), z.lang@sheffield.ac.uk (Zi-Qiang Lang)

The authors would like to acknowledge that this research work was supported by European Commission Seventh Framework Programme ENERGY.2012.2.3.2 under Grant Agreement Number 322430

Conflict of interest - none declared

wind turbine or a subsystem of the wind turbine such as the generator and gearbox. The inputs are the external environmental conditions such as wind speed and ambient temperature, and the outputs are the physical variables affected by wind turbines operation such as power output and generator temperature. Hardware sensors are traditional sensors. Soft sensors are built off-line using the first principles or data-driven methods (Ge and Song, 2010; Shang et al., 2014). The outputs of hardware and soft sensors are individual signals. From the signals, features are extracted by signal processing techniques such as, e.g., Fourier transform and wavelet transform (Lu et al., 2009) for the purpose of condition monitoring and fault diagnosis. Instead, model sensors are built on-line to reveal the changes of the relationship between the input and output measurements in real time. Moreover, model sensors use a model to represent system health conditions and exploit model analysis techniques to extract the damage sensitive features (Yang et al., 2013; Peng et al., 2007).

Some researchers have already adopted the idea of the model sensor method for wind turbine fault detection. For example, Gill et al. (2012) used the SCADA data in a normal wind turbine to generate a baseline copula-power curve, which is the power curve transformed by the copula estimation; then the similarity between the copula-power curves in the actual turbine operating condition and the baseline case is evaluated for the purpose of wind turbine fault detection. Yang et al. (2013) trained 4$^{\text{th}}$ degree polynomial models to describe the relationship between the SCADA parameters under both healthy and faulty conditions. As this relationship varies with turbine health conditions, the model coefficients can be used as indicators for wind turbine fault detection. Zhang et al. (2020) established state model curves by the bin method with SCADA data for wind turbines. The health index based on the Euclidean distance between the baseline state model curve and the investigated state model curve are proposed for the wind turbine health monitoring. Long et al. (2015) described the power curve profile by a Weibull cumulative distribution function (WCDF)-based model, which contains two parameters. The SCADA data were partitioned into consecutive time intervals and each subset of data was used to train a power curve profile by a least-squares method. Through monitoring changes in the model parameters, the online wind turbine health monitoring was achieved. Pashazadeh et al. (2018) proposed to build an autoregressive (AR) model with the time series data from a wind turbine over a sliding window. In this method, the coefficients of the AR model are updated while the window is moving as time goes. The fault detection of the wind turbine is then implemented by monitoring the change of the AR model coefficients. In these cases, the copula-power curves, polynomial models, state model curves, WCDF-based models, and AR models can all be regards as model sensors for monitoring the health conditions of wind turbines. The damage sensitive model features (i.e. the characteristics of the copula-power curves, the coefficients of the polynomial models, the characteristics of the state model curves, the parameters of the WCDF-based models, and the coefficients of the AR models, respectively) rather than individual signals are used for the purpose of fault detection. These existing model sensors are mainly static model-based, which are independent from time.

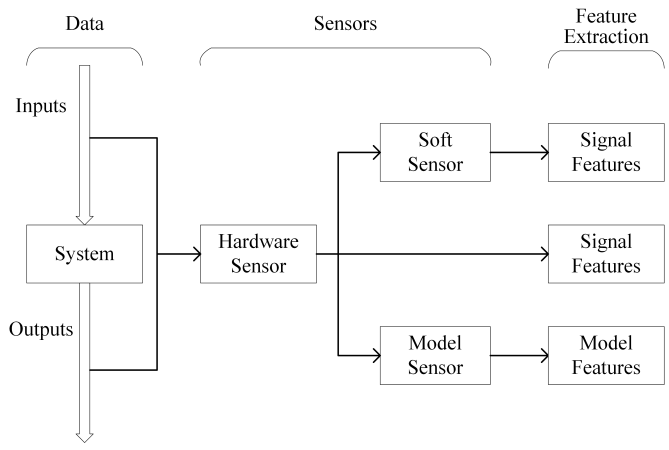

Fig. 1. Schematic diagram showing a comparison of hardware sensors, soft sensors, and model sensors.

The SCADA data of wind turbines include many measurements such as power output, generator temperature, gear box vibration, wind speed, and ambient temperature etc. The relationship between most of these are static. For example, the relationship between wind speed and power output is the widely used static power curve. Although gear box vibration varies much faster than the 10 min sampling rate of SCADA data, the associated SCADA measurement is the average of the vibration data over the 10 min, which is again statically related to other variables such as power output. However, it is observed that the relationship between wind speed, turbine ambient temperature, and generator temperature is dynamic and the dynamics can be fully covered by the 10 min per sample sampling rate. Considering a dynamic model can provide much richer information than a static one for system analysis, the dynamic relationship between the three variables will be used in the present study as a model sensor for the purpose of the wind turbine system fault diagnosis. The aim is to detect incipient wind turbine generator faults and provide wind farm operators with an early alarm when a failure is about to take place. Although there are abundant researches constructing the relationships between SCADA parameters through a black-box model (such as deep neural networks (Wang et al., 2017), Gaussian process models (Pandit and Infield, 2018)) where no prior knowledge is required, the grey-box models, which involve physical laws, can normally achieve better interpretability, are more parsimonious in terms of parameters, and have a better capability to deal with epistemic uncertainty (Worden et al., 2018). Considering this, in the present study, it is proposed that the dynamic relationship between wind speed, turbine ambient temperature, and generator temperature will first be derived using the first principles. Then, the parameters in the dynamic relationship will be regularly updated using a parameter estimation procedure to produce a model that can in real time reflect the changes in this dynamic relationship. After that, the damage sensitive features are extracted from the updated dynamic model to perform fault detection using a novel nonlinear system frequency analysis known as NOFRFs (nonlinear output frequency response functions) method. This

novel approach is then applied to process the SCADA data from 3 operating wind turbines over 5 years when a generator failure had taken place once in one of the 3 turbines. The results show that the new approach can reveal incipient generator fault occurring well before failure, demonstrating its significant potential in SCADA-data-based wind turbine fault detection and failure prognosis.

2. Dynamic model sensor for wind turbine fault detection

Fig. 2 illustrates the principle of the dynamic model sensor for the SCADA data-based wind turbine fault detection. Here, the time series data are the data of the wind speed, ambient temperature and generator temperature. These data are regularly collected from the SCADA system and used to update the parameters of a model sensor. The model sensor represents the dynamic relationship between the wind speed, ambient temperature, and generator temperature over the time when the data are collected. Therefore, from the analysis of the model sensor characteristics, the operational status of a wind turbine can be evaluated, and potential faults with the turbine system and components can be detected from a damage sensitive index as illustrated at the bottom of Fig. 2. The implementation of these ideas requires to address three issues which are the model sensor design, model sensor parameter updating, and model sensor analysis, respectively. The model sensor design and parameter updating are concerned with the determination of the model structure and parameters while the model sensor analysis is to extract model features and evaluate an index which is sensitive to wind turbine system and component damage for potential fault detection.

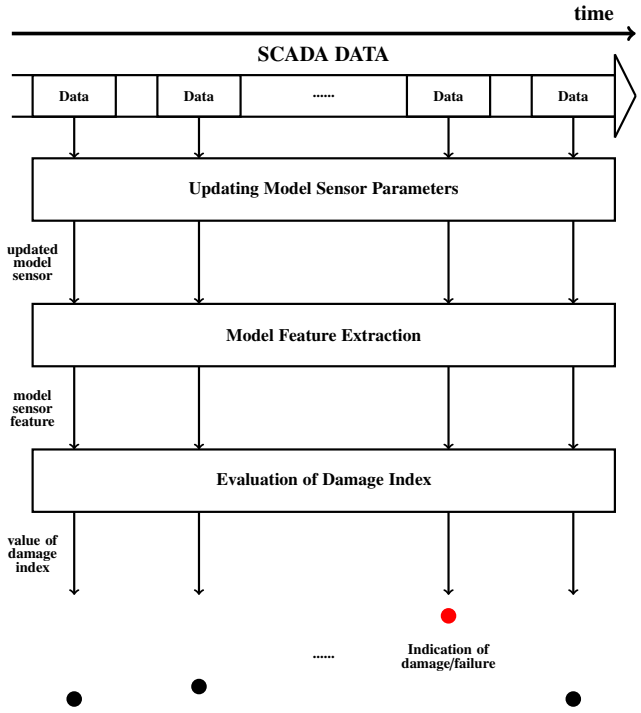

Fig. 2. Procedural of the model sensor method to detect the system changes.

3. Design and parameter update of the model sensor

3.1. Model sensor design

The first principles will be applied in the following to find the relationship between generator winding temperature, wind speed and ambient temperature to determine the model sensor structure. According to (Esfandiari and Lu, 2014), the relationship between the temperature change of the wind turbine generator winding ΔT_g(°C) and associated energy Q(J) is given by

$$Q = C_g \Delta T_g = C_g(T_g(k) - T_g(k-1)) \tag{1}$$

where C_g is the thermal capacitance (J/°C), $k \in \mathbb{Z}^+$ denotes the discrete time, and $T_g(k)$ is the generator winding temperature at the k^{th} time instant.

The energy Q can be determined by the "energy in" Q_{in} caused by copper loss (Aglen, 2003), and the "energy out" Q_{out} caused by cooling, that is

$$Q = Q_{in} - Q_{out}. \tag{2}$$

Copper loss is the heat produced by the current in generator windings, and Q_{in} generally has a nonlinear relationship with the wind speed denoted as V_w. It is found that a third-degree polynomial is sufficient to approximate this relationship (Tamura, 2012). In addition, as there is no copper loss when wind speed is 0, the constant term in the polynomial is 0; therefore, the polynomial is given by

$$Q_{in} = f(V_w) = f_3 {V_w}^3 + f_2 {V_w}^2 + f_1 V_w. \tag{3}$$

For Q_{out}, we only consider the conduction effect between the external environment and the generator, and the thermal resistance (°C/W) between them is denoted as R_{ga}. The equation of the heat conduction is given by (Esfandiari and Lu, 2014)

$$Q_{out} = t_s q_{out} = t_s \frac{T_g - T_a}{R_{ga}} \tag{4}$$

where q_{out} is the heat flow rate (W), $t_s = 600$ s is the time interval of the SCADA data collection, R_{ga} is thermal resistance, and T_a is the ambient temperature (°C).

The generators often have a cooling system which is composed of the blades directly mounted onto the generator rotor shaft. Therefore, R_{ga} is determined by generator rotor speed. The fan speed is generally proportional to $1/R_{ga}$, and the relationship between the rotor speed and the wind speed can be approximated by a third-degree polynomial (Shin et al., 2010). Thus, the relationship between the thermal resistance and the wind speed is described by

$$\frac{1}{R_{ga}} = g(V_w) = g_3 {V_w}^3 + g_2 {V_w}^2 + g_1 V_w + g_0. \tag{5}$$

According to (1)-(5), the dynamic model representing the generator winding temperature can be written as

$$T_g(k) = \frac{C_g^{-1} f(V_w(k)) + T_g(k-1) - T_a(k)}{1 + C_g^{-1} t_s g(V_w(k))} + T_a(k). \tag{6}$$

3.2. Model sensor parameter updating

In order to apply the dynamic model (6) to SCADA data for wind turbine fault detection in real time, the parameters of the model need to be updated regularly. The prediction error minimization (PEM) method (Söderström and Stoica, 1989) is applied to update the parameters of model (6). The use of the PEM method is based on the relationship

$$\begin{aligned} T_g^*(k) =& \frac{C_g^{-1} f(V_w^*(k)) + T_g^*(k-1) - T_a^*(k)}{1 + C_g^{-1} t_s g(V_w^*(k))} \\ &+ T_a^*(k) + e(k) \\ \triangleq& \hat{T}_g(k) + e(k) \end{aligned} \tag{7}$$

where $T_g^*(k)$, $V_w^*(k)$ and $T_a^*(k)$ are the generator temperature, wind speed and ambient temperature measured by the SCADA system, $e(k)$ is the modelling error. Considering (3) and (5), $\hat{T}_g(k)$ can be written as

$$\begin{aligned} &\hat{T}_g(k) = \\ &\frac{C_g^{-1}(f_3 {V_w^*}^3(k) + f_2 {V_w^*}^2(k) + f_1 V_w^*(k)) + T_g^*(k-1) - T_a^*(k)}{1 + C_g^{-1} t_s (g_3 {V_w^*}^3(k) + g_2 {V_w^*}^2(k) + g_1 V_w^*(k) + g_0)} \\ &+ T_a^*(k). \end{aligned} \tag{8}$$

In order to estimate the parameters of the model sensor, PEM minimizes the square of the prediction error such that

$$\min_{\theta} \sum_{k=1}^{N_s} F_k^2(\theta) \tag{9}$$

where N_s is the sample size,

$$\begin{aligned} &F_k(\theta) = \hat{T}_g(k) - T_g^*(k) \\ =& \frac{C_g^{-1}(f_3 {V_w^*}^3(k) + f_2 {V_w^*}^2(k) + f_1 V_w^*(k)) + T_g^*(k-1) - T_a^*(k)}{1 + C_g^{-1} t_s (g_3 {V_w^*}^3(k) + g_2 {V_w^*}^2(k) + g_1 V_w^*(k) + g_0)} \\ &- \left(T_g^*(k) - T_a^*(k)\right) \end{aligned} \tag{10}$$

and

$$\begin{aligned} \theta =& [\theta_1, \ldots, \theta_7]^{\mathrm{T}} \\ =& C_g^{-1}\left[f_3, f_2, f_1, t_s g_3, t_s g_2, t_s g_1, 1/C_g^{-1} + t_s g_0\right]^{\mathrm{T}} \end{aligned} \tag{11}$$

is the vector of model sensor parameters to be updated regularly for the purpose of wind turbine fault detection. After the parameter vector θ has been obtained, the dynamic model sensor, according to (8), is given by

$$\begin{aligned} &y(k) = \\ &\frac{\theta_1 {u_1}^3(k) + \theta_2 {u_1}^2(k) + \theta_3 u_1(k) + y(k-1) - u_2(k)}{\theta_4 {u_1}^3(k) + \theta_5 {u_1}^2(k) + \theta_6 u_1(k) + \theta_7} \\ &+ u_2(k) \end{aligned} \tag{12}$$

where $u_1 = V_w^*$ and $u_2 = T_a^*$ are model inputs and $y = \hat{T}_g$ is the model output.

3.3. Comparison with an existing model

A similar thermal dynamic model structure can be found in (Qiu et al., 2016), where the thermal resistant is assumed as a constant. The model fitting performance of the constant thermal resistance model in (Qiu et al., 2016) and wind speed dependent thermal resistance model (6) is compared in Fig. 3. Two different cooling processes are shown in the figure in the top and bottom plots, respectively. In both processes, the wind turbine is shut down at about 1300 minutes, then the generator starts cooling down. It is found that for the model with a constant thermal resistance, the model predicted cooling process is slower than the real system at the beginning, but faster at the end. The reason of the mismatch is because that the cooling system still works at the beginning of the cooling process, until the generator rotor shaft is totally stopped. The thermal resistance of the real system unceasingly increases with the rotor speed slowdown in the cooling process. However, the proposed model (6) of a wind speed dependent thermal resistance obviously produces a much better representation for the generator cooling process.

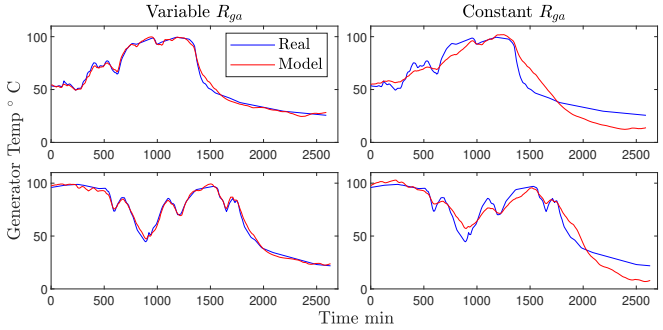

Fig. 3. Model fitting performance of the constant and wind speed dependent thermal resistance models for the cooling processes.

4. Extraction of damage sensitive features of model sensor using NOFRFs

To quantitatively evaluate the characteristics of the model sensor for fault detection, the damage sensitive features should be extracted from each updated model sensor. The model parameters can be the features in some cases, but the number of the parameters involved in model sensor (12) implies the parameters are hard to be used to produce a simple index for the fault detection objective. The frequency features of a system model are often very effective features for the representation of system properties (Frank, 1990). When a model is nonlinear, the nonlinear output frequency response functions (NOFRFs) have been demonstrated to be effective for the frequency feature extraction and analysis (Peng et al., 2011, 2007). Therefore, the NOFRFs will be exploited here for the extraction of the model sensor features for wind turbine fault detection.

4.1. The Volterra series representation of the model sensor

When wind speed varies around V_w^0 and turbine ambient temperature varies around T_a^0, the model sensor (12) is known as

being working around the operating point $\left(V_w^0, T_a^0\right)$. If the variation of the turbine ambient temperature about T_a^0 is negligible, the system (12) is subject to inputs

$$\begin{aligned} u_1(k) &= u(k) + V_w^0 \\ u_2(k) &= T_a^0. \end{aligned} \tag{13}$$

As input u_2 is a constant, system (12) can be regarded as a single input and single output system which has input $u(k)$ and output $y(k)$. The underlying continuous single-input-single-output system can be represented by the Volterra series as follows

$$y(t) = h_0 + \sum_{n=1}^{N} \int_{-\infty}^{\infty} \cdots \int_{-\infty}^{\infty} h_n(\tau_1, \ldots, \tau_n) \prod_{i=1}^{n} u(t - \tau_i) d\tau_i \tag{14}$$

where h_0 is a stable equilibrium of the system, $h_n(\tau_1, \ldots, \tau_n)$ is the n^{th} order Volterra kernel, and N denotes the maximum order of the system nonlinearity. Fig. 4 illustrates this representation of model sensor system (12).

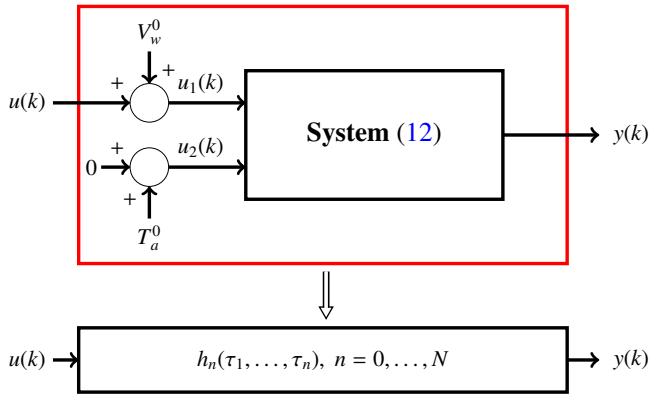

Fig. 4. The Volterra series representation of the model sensor (12).

4.2. The NOFRFs

The NOFRFs are proposed based on the Volterra series representation of a nonlinear system. The output frequency response of system (14) can be described as (Lang and Billings, 2005)

$$Y(j\omega) = \sum_{n=0}^{N} Y_n(j\omega), \tag{15}$$

where

$$\begin{aligned} Y_0(j\omega) &= \begin{cases} h_0 & \text{for} \quad \omega = 0 \\ 0 & \text{for} \quad \omega \neq 0 \end{cases} \\ Y_n(j\omega) &= \frac{1/\sqrt{n}}{(2\pi)^{n-1}} \int_{\omega_1 + \cdots + \omega_n = \omega} H_n(j\omega_1, \ldots, j\omega_n) \prod_{i=1}^{n} U(j\omega_i) d\sigma_{n\omega}. \end{aligned} \tag{16}$$

and

$$\begin{aligned} H_n(j\omega_1, \ldots, j\omega_n) = \int_{-\infty}^{\infty} \cdots \int_{-\infty}^{\infty} h_n(\tau_1, \ldots, \tau_n) \\ \times e^{-j(\omega_1\tau_1 + \cdots + \omega_n\tau_n)} d\tau_1 \ldots d\tau_n \end{aligned} \tag{17}$$

is known as the n^{th} order generalised frequency response function (GFRF), which is a description of the characteristics of nonlinear systems in the frequency domain. In (16),

$$\int_{\omega_1 + \cdots + \omega_n = \omega} H_n(j\omega_1, \ldots, j\omega_n) \prod_{i=1}^{n} U(j\omega_i) d\sigma_{n\omega} \tag{18}$$

denotes the summation of $H_n(j\omega_1, \ldots, j\omega_n) \prod_{i=1}^{n} U(j\omega_i)$ over the n-dimensional hyperplane $\omega_1 + \cdots + \omega_n = \omega$.

For $n = 0, 1, \ldots, N$, the spectrum of the $u^n(k)$ at the frequency ω is given by (Lang and Billings, 2005)

$$\begin{aligned} U_0(j\omega) &= \begin{cases} 1 & \text{for} \quad \omega = 0 \\ 0 & \text{for} \quad \omega \neq 0 \end{cases} \\ U_n(j\omega) &= \frac{1/\sqrt{n}}{(2\pi)^{n-1}} \int_{\omega_1 + \cdots + \omega_n = \omega} \prod_{i=1}^{n} U(j\omega_i) d\sigma_{n\omega}. \end{aligned} \tag{19}$$

Thus, we can define the n^{th} order nonlinear output frequency response function (NOFRF) at frequency ω as

$$G_n(j\omega) = \frac{Y_n(j\omega)}{U_n(j\omega)} \tag{20}$$

under the condition

$$U_n(j\omega) \neq 0. \tag{21}$$

Therefore, $Y_n(j\omega)$ in (15) can be expressed as

$$Y_n(j\omega) = G_n(j\omega) U_n(j\omega). \tag{22}$$

Consequently, the output frequency response of system (14) can be represented using the NOFRFs as

$$Y(j\omega) = \sum_{n=0}^{N} G_n(j\omega) U_n(j\omega). \tag{23}$$

The condition (21) implies that the NOFRF $G_n(j\omega)$ only exists when $U_n(j\omega) \neq 0$. As $U_0(j\omega)$ is non-zero only at 0 frequency, we can use G_0 to stand for $G_0(j\omega)$. In addition, based on the definition (20), G_0 is identical to the system's stable equilibrium h_0.

4.3. Evaluation of the NOFRFs under harmonic inputs

In the present study, harmonic inputs with frequency $\omega_c \neq 0$ will be used to excite the model sensor for the NOFRFs evaluation. In this case, the system output only contains frequency components at $\{p\omega_c | p = 0, 1, \ldots, N\}$, and according to (Peng et al., 2007), the output frequency response of system (23) can now be described as

$$Y(jp\omega_c) = \sum_{i=0}^{q} G_{p+2i}(jp\omega_c) U_{p+2i}(jp\omega_c) \tag{24}$$

where $q = \lfloor (N - p)/2 \rfloor$. When a nonlinear system is subject to a harmonic input, the existence of the NOFRFs over different frequencies is shown in Table 1.

Table 1. The existence of NOFRFs over different frequencies when a nonlinear system is subject to harmonic input with 1 indicating existence and 0 nonexistence.

Ω \ G	$G_0(j\Omega)$	$G_1(j\Omega)$	$G_2(j\Omega)$	$G_3(j\Omega)$	$G_4(j\Omega)$	$\cdots$
0	1	0	1	0	1	$\cdots$
ω_c	0	1	0	1	0	$\cdots$
$2\omega_c$	0	0	1	0	1	$\cdots$
$3\omega_c$	0	0	0	1	0	$\cdots$
$\vdots$	0	0	0	0	$\vdots$	$\vdots$

The NOFRF $G_n(j\omega)$ is insensitive to the change of the input by a constant factor α ($\alpha \neq 0$) (Lang and Billings, 2005), that is,

$$G_n(j\omega)|_{u(t)=u^*(t)} = G_n(j\omega)|_{u(t)=\alpha u^*(t)}. \tag{25}$$

Thus, if the model is excited by the harmonic input $u^*(t)$ scaled by $\bar{N}$ different constants $\alpha_1, \alpha_2, \cdots, \alpha_{\bar{N}}$, respectively, to produce $\bar{N}$ different system frequency responses $Y^i(j\omega)$, $i = 1, \ldots, \bar{N}$, the following equation can be obtained.

$$\mathbf{Y}(jp\omega_c) = \mathbf{AU}(jp\omega_c)\mathbf{G}(jp\omega_c) \tag{26}$$

where

$$\begin{aligned}
\mathbf{Y}(jp\omega_c) &= \left[Y^1(jp\omega_c), Y^2(jp\omega_c), \ldots, Y^{\bar{N}}(jp\omega_c)\right]^{\mathrm{T}} \\
\mathbf{AU}(jp\omega_c) &= \begin{bmatrix} U_p^1(jp\omega_c) & U_{p+2}^1(jp\omega_c) & \cdots & U_{p+2q}^1(jp\omega_c) \\ U_p^2(jp\omega_c) & U_{p+2}^2(jp\omega_c) & \cdots & U_{p+2q}^2(jp\omega_c) \\ \vdots & \vdots & \ddots & \vdots \\ U_p^{\bar{N}}(jp\omega_c) & U_{p+2}^{\bar{N}}(jp\omega_c) & \cdots & U_{p+2q}^{\bar{N}}(jp\omega_c) \end{bmatrix} \\
\mathbf{G}(jp\omega_c) &= \left[G_p(jp\omega_c), G_{p+2}(jp\omega_c), \ldots, G_{p+2q}(jp\omega_c)\right]^{\mathrm{T}}
\end{aligned} \tag{27}$$

and $U_n^i(jp\omega_c)$, $i = 1, \ldots, \bar{N}$, $n = 0, \ldots, N$ is the spectrum of the input $(\alpha_i u^*(k))^n$ at the frequency $p\omega_c$. To avoid (26) to be underdetermined, it is required that $\bar{N} \geq q + 1$. Consequently, the NOFRFs of nonlinear systems subject to a harmonic input can be determined as

$$\mathbf{G}(jp\omega_c) = \left[\mathbf{AU}(jp\omega_c)^{\mathrm{T}}\mathbf{AU}(jp\omega_c)\right]^{-1}\mathbf{AU}(jp\omega_c)^{\mathrm{T}}\mathbf{Y}(jp\omega_c) \quad p = 0, 1, \ldots N. \tag{28}$$

4.4. Damage sensitive indices

As the Volterra series representation shown in Fig. 4 is dependent on the operating point $\left(V_w^0, T_a^0\right)$, the NOFRFs of the model sensor (12) evaluated using the method in Section 4.3 above will be affected by $\left(V_w^0, T_a^0\right)$. Therefore, when the NOFRFs of the investigated wind turbine are compared with the NOFRFs of other turbines in the wind farm, the two wind turbines should be at the same operating point $\left(V_w^0, T_a^0\right)$ for the purpose of wind turbine fault detection. Denote the NOFRFs of model sensor (12) and their baseline that represent the current and normal conditions of a wind turbine working about the operating point $\left(V_w^0, T_a^0\right)$ as $G_n(j\omega)$ and $G_n^b(j\omega)$, $n = 0, \ldots, N$, respectively. Then, the NOFRFs based damage sensitive indices for the wind turbine can be defined as

$$I_n(j\omega) = |G_n(j\omega)| - \left|G_n^b(j\omega)\right|, \quad n = 0, \ldots, N. \tag{29}$$

In principle, $G_n^b(j\omega)$ is the NOFRF determined from a benchmark wind turbine which is similar to the evaluated turbine system and is working normally in a similar environment.

In practical applications, $M (M \geq 2)$ wind turbines in the same wind farm and located near the wind turbine of concern can be used as the benchmark and, each time, the values of indices (29) are evaluated. Obviously, in most cases, when an alarm is raised from the evaluated values of (29), there are two possible situations. One is the benchmark is normal, so the alarm correctly indicated there exists a fault with the wind turbine of concern. Another is the benchmark turbine is of fault so the alarm may be wrong. It is assumed that at the same time greater than 50% of the benchmark wind turbines can be normal. Therefore, if greater than 50% of the evaluated values of index (29) indicate there exists a fault, the turbine of concern can be considered to be fault. Otherwise, the turbine can be normal. Thus, the SCADA data based wind turbine fault detection can be achieved.

In some special cases, such as grid failure event or storm, it is possible that more than 50% wind turbines can simultaneously show abnormal behaviours in some measurements such as power output and generator temperature. In these cases, given the severity of the problems, it is expected that the abnormality would be easily identified by the alarm system embedded in the wind turbines. Consequently, in response to the alarm by the embedded system, the proposed approach can stop working until the alarm has been lifted indicating most turbines have now performed normally.

4.5. Model sensor based wind turbine generator fault detection

Based on the model sensor design in Section 3 and the NOFRF based model feature extraction introduced above, a detailed algorithm for the SCADA dada-based wind turbine fault detection can be summarised as follows.

1. Take the wind turbine of concern for fault detection as the turbine to be assessed and the other turbines in the wind farm with operating environments similar to that of the turbine to be assessed as benchmarks.
2. At the beginning of every day, the parameters of the model sensor (12) are updated using PEM method and the SCADA data over the latest 30 days for each wind turbine.
3. Evaluate the output response of the model sensor for each wind turbine to $\bar{N}$ different harmonic inputs
$$u(t) = \alpha_i u^*(t), \quad i = 1, 2, \ldots, \bar{N}. \tag{30}$$
4. Evaluate the Fourier transform of the model sensor outputs and corresponding inputs and construct $\mathbf{Y}(jp\omega_c)$ and $\mathbf{AU}(jp\omega_c)$ in equation (27) for each wind turbine.
5. Evaluate the NOFRFs of the model sensor for each wind turbine using equation (28).

6. Evaluate the damage sensitive indices (29) with $G_n(j\omega)$ representing the NOFRF of the wind turbine to be assessed and $G_n^b(j\omega)$ representing the NOFRF of a benchmark turbine
7. Raise alarm if the damage sensitive indices evaluated for more than 50% benchmark wind turbines exceed a threshold then get back to step 1 and repeat steps 1-6 when a new day starts.

5. Application to fault detection of an operating wind turbine

5.1. The SCADA data description

The data used in the present study were collected from the SCADA of three operating wind turbines which are referred to as A101, A102 and A103, respectively. The three wind turbines are of the same model and located close to each other in a wind farm in Spain. The data were collected from 01/08/2009 to 31/12/2014. Every 10 minutes, 40 measurements were obtained from each turbine. These measurements include the wind speed, the temperature of various components, the vibration of the tower, and the power output, etc. The maximum, minimum, standard deviation and average of the measurements over the 10 minutes were recorded. The SCADA measurements used in this study are listed in Table 2.

Table 2. The SCADA measurements used in this study.

Sensor Measurement	Symbol	Units
Wind speed	V_w	m/s
Ambient temperature	T_a	°C
Generator temperature	T_g	°C
Power output	P_o	kW
Blade 1 pitch angle	B_1	deg(°)
Blade 2 pitch angle	B_2	deg(°)
Blade 3 pitch angle	B_3	deg(°)

In 01/2013, the generator of turbine A103 was replaced for a serious rotor winding failure, which is shown in Fig. 5. The generator failure was detected by an operator with a wave comparator on 21/01/2013, but the SCADA system failed to detect this failure. Then the wind turbine was recovered after a new generator was installed on 22/01/2013.

Fig. 5. Rotor winding short circuit causing the generator failure of wind turbine A103 in 01/2013.

5.2. The SCADA data pre-processing

In this application study, the model sensor technique proposed in Sections 3 to 4 is applied to process the SCADA data in order to demonstrate how to use the proposed technique to detect the generator failure in advance. For this purpose, the SCADA data were first pre-processed to clean the data by 1) removing the data sets which have missing data and outliers, and 2) setting wind speed as 0 when wind turbine stopped.

A considerable proportion of missing values were found from the SCADA data. For example, 2.15% power data during 01/08/2009 to 31/12/2014 from wind turbine A103 are missing. Data set with missing data cannot be used for model sensor parameter updating, so have to be removed. The data set with outliers may affect the accuracy of model parameter estimation so should also be removed. The rules of the outlier detection are shown in Table 3. The first type of outlier is simply detected by whether the average or standard deviation of the parameters are beyond the normal ranges. The second type of outlier is that the environment parameters, i.e. wind speed and ambient temperature, stay at a constant value or increase/decrease linearly, which can be detected by checking whether the standard deviation of the parameters has been unchanged for a long time. The examples of the second type outlier are shown in Fig. 6. In Outlier 1, σ_{V_w} stays at 0 for about 10000 minutes (or 7 days), and correspondingly V_w stays at the low speed 0.4 m/s. In Outlier 2, σ_{V_w} stays at 0.0025 for about 4500 minutes (or 3 days), and meanwhile, V_w linearly increases from 9 to 13 m/s. As a linear change of the wind speed or ambient temperature is unlikely in practice, the data are the outliers. The third type of outlier is caused by blade pitch control. The pitch control affects the wind turbine power output especially when the wind speed exceeds the rated wind speed or the curtailment happens. Fig. 7 shows a comparison between the entire power curve and the power curve when the pitch angle is larger than 10 degree. After the wind speed exceeds the rated wind speed, the curtailment can cause the power output to be slightly lower than the rated power or to be zero. The first type of the curtailment is treated as outlier, while the second type is treated as wind turbine stop.

The data measured when wind turbines stopped have been kept, since the data can help to model the cooling processes. Wind turbines may be shut down when wind speed was beyond the range between cut-in (3 m/s) and cut-off (25 m/s) wind speed or the turbine was in the second type of curtailment shown in Fig. 7. In both cases, no power was produced, and the generator was cooling down. As the wind speed has no effect on power output or generator temperature when a wind turbine stops, the wind speed is taken as 0 in the data analysis.

5.3. Power curve analysis

The traditional power curve analysis was first applied to the SCADA data of wind turbine A103, which is shown in Fig. 8. As the data were pre-processed according to Section 5.2, the

Table 3. The rules of the outlier detection. σ_{V_w}, σ_{T_g}, and σ_{T_a} are the standard deviation of the wind speed, the generator temperature, and the ambient temperature, respectively. B_1, B_2, B_3 are the pitch angles (in degrees) of the three blades.

Outlier category	Detection rule
Threshold exceeded	1. $\sigma_{V_w} > 20$ 2. $\sigma_{T_g} > 5$ or $T_g > 150$ or $T_g < 0$ 3. $\sigma_{T_a} > 5$ or $T_a > 50$ or $T_a < -10$
No change or linear increase/decrease in environmental parameters	1. σ_{V_w} has not changed for more than 50 minutes. 2. σ_{T_a} has not changed for more than 1500 minutes.
Pitch controlled	B_1 or B_2 or $B_3 > 10$ when power output is not 0.

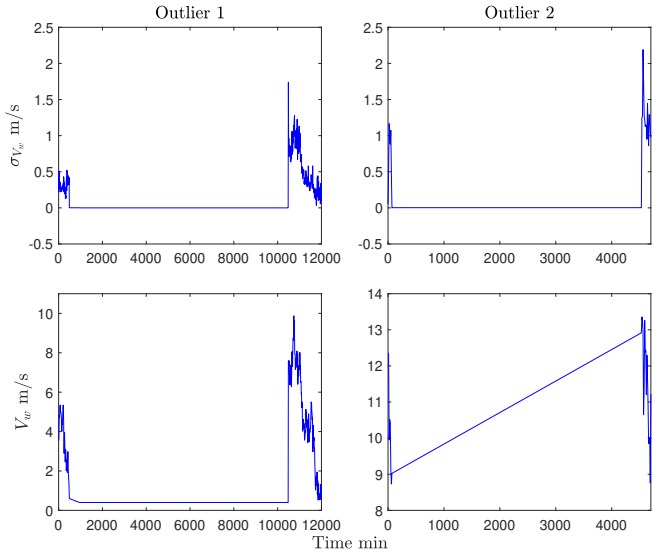

Fig. 6. An illustration of the second type of outlier.

wind speed is set as 0 when no power is generated. Therefore, the power curve in some wind speed ranges, e.g. between 0 and cut-in wind speed, are missing. The wind speed from 0 to 25 m/s were divided into 25 bins with a 1 m/s interval, and the mean value of each bin was evaluated. Through comparing the power curves in January over the three years before the failure happened, no significant change has been observed.

5.4. *Analysis of the generator temperature*

The generator temperature of the three wind turbines are compared in Fig. 9. The data plotted has been pre-processed according to Section 5.2. As the three wind turbines were under similar environmental conditions, the generator temperature data are close to each other. The left figure shows the raw SCADA data during the last 30 days just before the failure happens. Although the failure was about to happen, it is hard to distinguish the difference between the failure wind turbine and the normal wind turbines through the generator temperature data. The similar difficulty can also be found from the right figure, which is constructed by a moving average of the generator temperature over a sliding window of length 30 days with an one day step. The data used for computing the average on each day

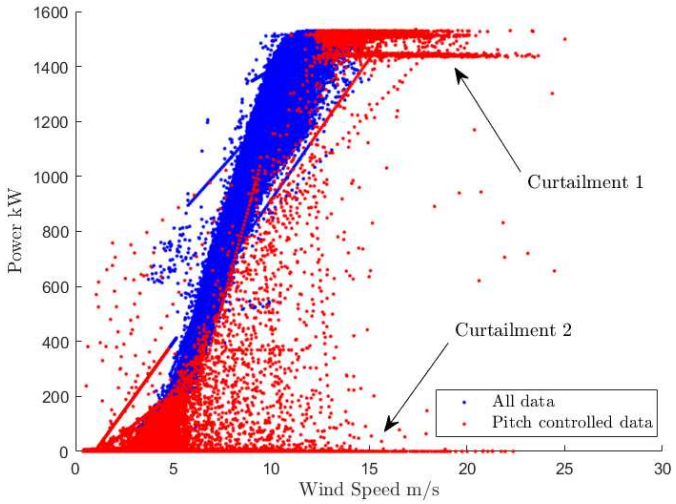

Fig. 7. The pitch controlled data in power curve and two types of curtailment.

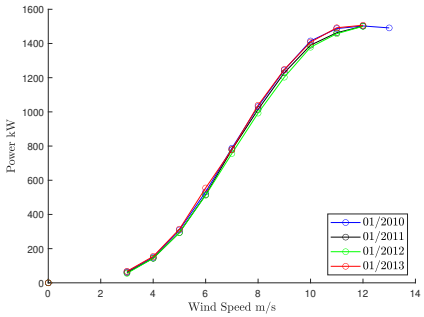

Fig. 8. Comparison of the power curve of 01/2013 with the power curves of 01/2010, 01/2011, and 01/2012.

is the same as the data used for model sensor update. From Fig. 9, it is obvious that the generator temperature data provide no any indication of the ageing process of the generator of turbine A103 and can therefore not be used for detection of the turbine winding damage.

5.5. *Application of the model sensor method to the wind turbine fault detection*

In this application, model sensor (12) was adopted. The model sensor parameters are updated every day for turbine A101, A102, and A103, respectively. In each updating, the data over 30 days are used, which, after pre-processing, contain about 4000 samples of data. For A103, as the new generator was installed on 22/01/2013, after the model sensor is updated on 21/01/2013, the next model sensor is updated on 20/02/2013, so that the 30 days' data are only from the new generator. From the data collected from the three turbines every day, three model sensors of the form of equation (12) are determined and used to represent the operating conditions of the three wind turbines, respectively. For example, the model sensor for A102 during

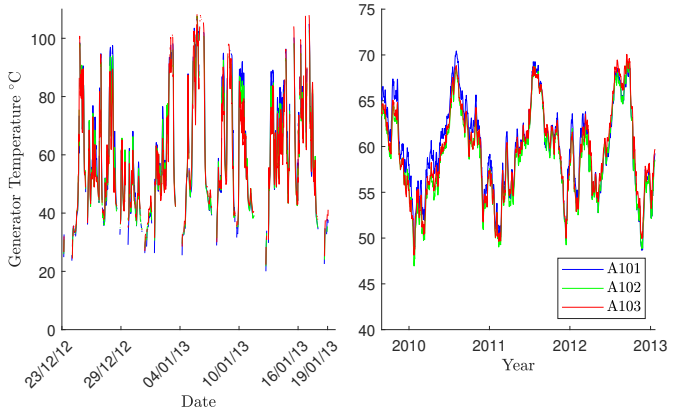

Fig. 9. The comparison between the three wind turbines in generator temperature. The left figure shows the generator temperature data from 23/12/2012 to 21/01/2013. The right figure shows the moving average from 30/08/2009 to 21/01/2013.

01/09/2009 to 30/09/2009 was obtained as follows.

$$y(k) = \frac{-0.0050u_1{}^3(k) + 0.1233u_1{}^2(k) + 0.0499u_1(k) + y(k-1) - u_2(k)}{2.9632\times10^{-4}u_1{}^3(k) - 0.0093u_1{}^2(k) + 0.0940u_1(k) + 0.8248} + u_2(k). \tag{31}$$

In order to evaluate the NOFRFs of the model sensors, the operating point of $(6.3, 21.7)$ was used where 21.7 °C is the average ambient temperature in the 30 days, while 6.3 m/s is the average wind speed over 01/08/2009 to 31/12/2014. Therefore, the inputs of model sensor (12) that were used for the evaluation of the NOFRFs are given by

$$\begin{aligned} u_1(k) &= u(k) + 6.3 \\ u_2(k) &= 21.7. \end{aligned} \tag{32}$$

Take

$$u(k) = \alpha u^*(k) \tag{33}$$

where $u^*(k) = \cos(\omega_c k t_s)$, and $\omega_c = 7.27\times10^{-5}$rad/s, which corresponds to the period of one day and is an important frequency component in the spectra of wind turbine SCADA measurements. As the sampling period of the SCADA system (i.e. 10 min) is much shorter than one day, the sampling frequency of the SCADA system is sufficient to capture the system dynamics at ω_c. Although in this case, the NOFRFs at a single frequency are evaluated, the NOFRFs can generally be evaluated at any frequencies of concern to assess the properties of a system under study.

The NOFRFs of model sensor (12) determined from SCADA data from a wind turbine were evaluated using (28) from $u(k)$ given by (33) and corresponding output $y(k)$ generated by the model sensor (31). The NOFRFs up to the 2nd order, i.e. G_0, $G_2(0)$, $G_1(j\omega_c)$ and $G_2(j2\omega_c)$) were used to assess the wind turbine operating conditions.

For example, in order to evaluate $G_1(j\omega_c)$, the maximum order of system nonlinearity was taken as $N = 6$ which implies the input $u^*(k)$ should be scaled by at least 3 different α (i.e. $\bar{N} \geq 3$). In this case, following the procedure in Section 4.3, three responses of model sensor (12) to $u(k) = \alpha_1 u^*(k) = 0.25u^*(k)$, $u(k) = \alpha_2 u^*(k) = 0.35u^*(k)$ and $u(k) = \alpha_3 u^*(k) = 0.5u^*(k)$, respectively, were used to determine $G_1(j\omega_c)$ as

$$\begin{aligned} G_1(j\omega_c) &= [1,0,0]\begin{bmatrix} G_1(j\omega_c) \\ G_3(j\omega_c) \\ G_5(j\omega_c) \end{bmatrix} \\ &= [1,0,0]\left[\mathbf{AU}(j\omega_c)^{\mathrm{T}}\mathbf{AU}(j\omega_c)\right]^{-1}\mathbf{AU}(j\omega_c)^{\mathrm{T}}\mathbf{Y}(j\omega_c) \\ &= 4.3332 - 1.5199j \end{aligned} \tag{34}$$

where

$$\begin{aligned} \mathbf{Y}(j\omega_c) &= \begin{bmatrix} Y^1(j\omega_c) \\ Y^2(j\omega_c) \\ Y^3(j\omega_c) \end{bmatrix} = \begin{bmatrix} 0.5416 - 0.1900j \\ 0.7581 - 0.2659j \\ 1.0827 - 0.3798j \end{bmatrix} \\ \mathbf{AU}(j\omega_c) &= \begin{bmatrix} U_1^1(j\omega_c) & U_3^1(j\omega_c) & U_5^1(j\omega_c) \\ U_1^2(j\omega_c) & U_3^2(j\omega_c) & U_5^2(j\omega_c) \\ U_1^3(j\omega_c) & U_3^3(j\omega_c) & U_5^3(j\omega_c) \end{bmatrix} \\ &= \begin{bmatrix} 0.1250 & 0.0015 & 0 \\ 0.1750 & 0.0040 & 0.0001 \\ 0.2500 & 0.0117 & 0.0006 \end{bmatrix} \end{aligned} \tag{35}$$

Similarly, G_0, $G_2(0)$, and $G_2(j2\omega_c)$) can also be obtained. Theoretically, the values of α can be chosen arbitrarily. However, if the model nonlinearity is significant, α greater than 1 will introduce a large input to the model, which may drive the system states into an unstable regime or a regime around another equilibrium. So, a good practice is to choose an α between 0 and 1.

In this study, A101 and A102 were used as the benchmark turbines. Therefore $M = 2$, and the M sets of damage sensitive indices for A103 are given by

$$\begin{cases} I_0^{A101} = \left|G_0^{A103}\right| - \left|G_0^{A101}\right| \\ I_1^{A101}(j\omega_c) = \left|G_1^{A103}(j\omega_c)\right| - \left|G_1^{A101}(j\omega_c)\right| \\ I_2^{A101}(0) = \left|G_2^{A103}(0)\right| - \left|G_2^{A101}(0)\right| \\ I_2^{A101}(j2\omega_c) = \left|G_2^{A103}(j2\omega_c)\right| - \left|G_2^{A101}(j2\omega_c)\right| \end{cases} \tag{36}$$

and

$$\begin{cases} I_0^{A102} = \left|G_0^{A103}\right| - \left|G_0^{A102}\right| \\ I_1^{A102}(j\omega_c) = \left|G_1^{A103}(j\omega_c)\right| - \left|G_1^{A102}(j\omega_c)\right| \\ I_2^{A102}(0) = \left|G_2^{A103}(0)\right| - \left|G_2^{A102}(0)\right| \\ I_2^{A102}(j2\omega_c) = \left|G_2^{A103}(j2\omega_c)\right| - \left|G_2^{A102}(j2\omega_c)\right| \end{cases} \tag{37}$$

The values of the two sets of indices evaluated by applying the proposed model sensor technique to the SCADA data of A101, A102, and A103 over the period from 01/08/2009 to 31/12/2014 are shown in Fig. 10.

It can be observed from Fig. 10 that both I_0^{A101} and I_0^{A102} start from a point higher than 0, and then follow a trend which

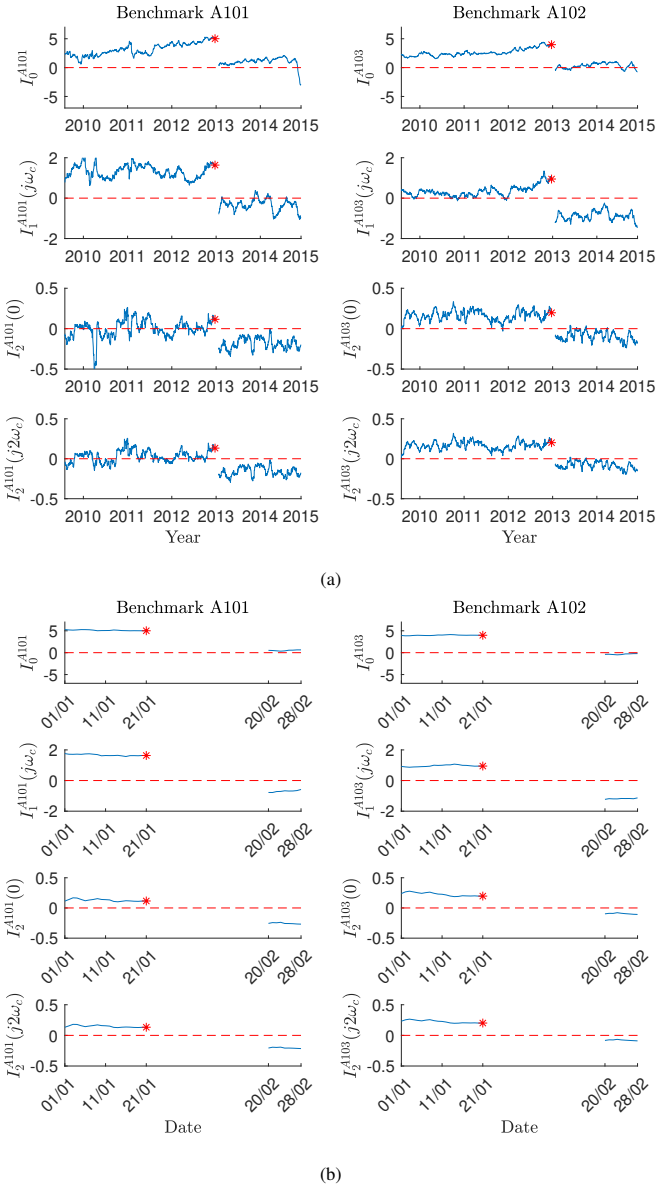

Fig. 10. The values of A103 damage sensitive indices I_0, $I_1(j\omega_c)$, $I_2(0)$, and $I_2(j2\omega_c)$) of the model sensor (12), with * indicating when the generator failure took place. The subfigure (a) shows the indices from 01/08/2009 to 31/12/2014 and (b) shows the zoomed-in results from 01/01/2013 to 28/02/2013.

slowly increases with time until the generator failure of A103 takes place in January 2013. After the time point when A103 generator was replaced, both I_0^{A101} and I_0^{A102} reduce back to about zero. These exactly reflect the actual operating conditions of wind turbine A103 and indicate that I_0 can be used as an excellent index for the SCADA data based wind turbine fault detection.

In addition, Fig. 10 shows that $I_1(j\omega_c)$ can also be a good index for the purpose of SCADA data based wind turbine fault detection. However, the trend with I_0, which slowly increases with time until the point when A103's failure took place, cannot be very obviously observed from $I_1(j\omega_c)$. The increasing trend of I_0 is important, as it is the evidence of the feasibility of the method to detect the incipient generator fault. Although only three wind turbines are available, the results achieved have demonstrated that the principle of the proposed method works and is expected to be applicable to more turbines.

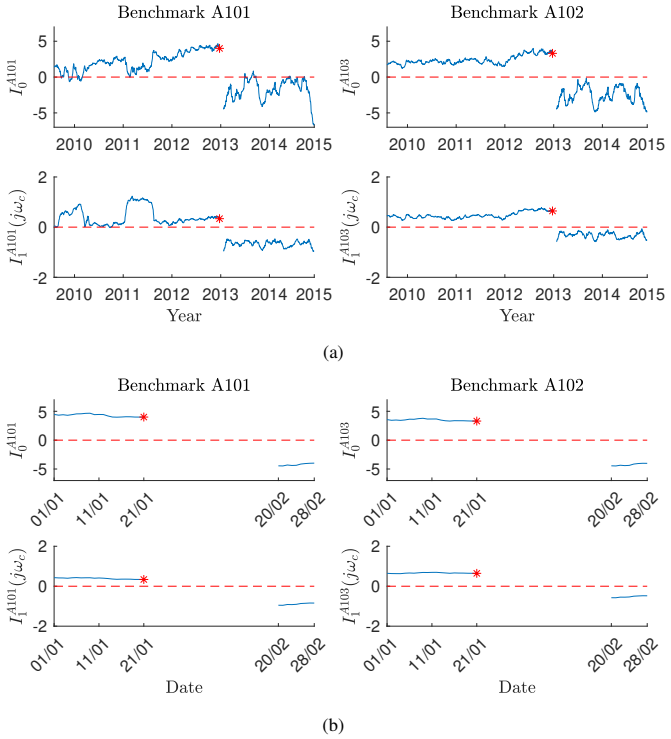

Fig. 11. The values of A103 damage sensitive indices I_0 and $I_1(j\omega_c)$ extracted from a linear model sensor (40), with * indicating when the generator failure took place. The subfigure (a) shows the indices from 01/08/2009 to 31/12/2014 and (b) shows the zoomed-in results from 01/01/2013 to 28/02/2013.

Also it is worth pointing out that although $G_2(0)$ and $G_2(j2\omega_c)$ cannot, as clearly as I_0, indicate the trend of change of the wind turbine operating status, it is still necessary to take the effect of system nonlinearity into account in the proposed analysis. If (3) and (5) are simplified as

$$\begin{aligned} f(V_w) &= f_1 V_w \\ g(V_w) &= g_0 \end{aligned} \tag{38}$$

the dynamic model (6) become linear, which is given by

$$T_g(k) = \frac{C_g^{-1} f_1 V_w(k) + T_g(k-1) - T_a(k)}{1 + C_g^{-1} t_s h_0} + T_a(k). \tag{39}$$

Following the steps in Section 3.2, the linear model sensor is given by

$$y(k) = \frac{\theta_1 u_1(k) + y(k-1) - u_2(k)}{\theta_2} + u_2(k) \tag{40}$$

Fig. 11 shows the results of I_0 and $I_1(j\omega_c)$ determined when assuming the linear model structure (39) so $N = 1$. It can be observed from Fig. 11 that I_0 thus obtained is not able to clearly show the trend of turbine winding ageing so as to properly issue an alarm before the winding failure takes place. In addition, $I_1(j\omega_c)$ obtained in this way is also obviously no longer a good index for the turbine operating conditions.

5.6. *Failure prognosis performance of the proposed model sensor approach*

In this section, the failure prognosis performance of the proposed approach will be evaluated.

From the values of I_0 in Fig. 10, it can be observed that the generator winding ageing damage was accumulated as time went by and eventually reached a level such that the generator failure took place on 21 January 2013. For the purpose of failure prognosis performance analysis, it is assumed that up to the date of 01/01/2012, the ageing damage accumulation with turbine A103 had been significant enough such that an incipient fault had occurred. Consequently, the generator conditions of A103 from 01/01/2012 to 21/01/2013 are labelled as faulty and the conditions over other times are labelled as normal. Thus, if a threshold for I_0 is set, the generator failure prognosis can be carried out by checking whether I_0 has exceeded the threshold. According to the algorithm summarised in Section 4.4, an alarm will be raised when the damage sensitive indices evaluated for more than 50% benchmark wind turbines exceed a threshold. As only two benchmark turbines are available in the present study, the prognosis analysis is carried out based on the following principle:

1. If the indices evaluated for both benchmark turbines have exceeded the threshold, an incipient fault is considered to have occurred indicating a failure is going to take place at a future time.
2. If the indices evaluated for one or none benchmark turbine have exceeded the threshold, no incipient fault is considered to have occurred indicating a failure is not going to take place at a future time.

From the results of the prognosis analysis thus conducted, the true positive rate (TPR) and false positive rate (FPR) can be worked out for each value of the threshold that has been used. Three examples of the threshold and the corresponding TPR and FPR are shown in Table 4 where the date when the prognosis decision could be made under each threshold is also provided. Clearly it can be observed from Table 4 that I_0 has good potential to detect an incipient fault and realises generator failure prognosis with a high TPR and low FPR. By choosing the threshold of I_0 over a range of values and carrying out corresponding failure prognosis analysis, a set of TPRs and FPRs can be obtained. The results are studied using the receiver operating characteristic (ROC) curve shown in Fig. 12. The area under the ROC curve (AUC) is 0.9882 indicating that the proposed model sensor approach has an excellent incipient fault detection/failure prognosis performance.

Table 4. The three thresholds of I_0 with their TPRs, FPRs, and the date of the first true positive alarm was raised.

Threshold	TPR	FPR	Date
3.0168	0.7390	0	04/03/2012
2.8243	0.8501	0.0104	27/02/2012
2.3077	1	0.2451	01/01/2012

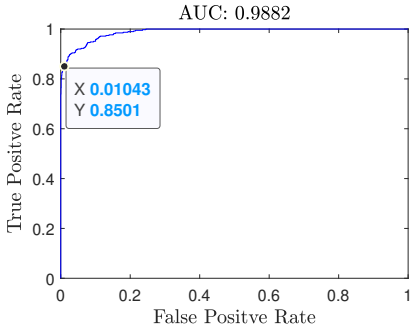

Fig. 12. The ROC curve of I_0, where the threshold of the data tip is 2.8243.

For the two normal wind turbines A101 and A102, when A102 is used as the benchmark of A101 and A101 as the benchmark of A102, the damage indices I_0^{A101} and I_0^{A102} are obtained are shown in Fig. 13. If the second threshold in Table 4 is adopted, it is found that, in both cases, I_0 is always below the threshold, so no false alarm will be raised.

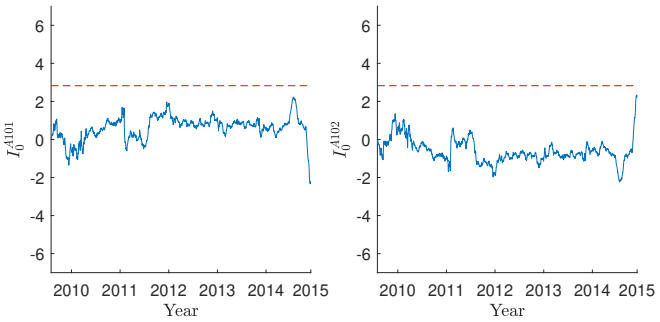

Fig. 13. The values of A102 damage sensitive indices I_0^{A101} when A101 wind turbine is the benchmark and the values of A101 damage sensitive indices I_0^{A102} when A102 wind turbine is the benchmark. The threshold is 2.8243.

6. Conclusions

In this paper, a novel dynamic model sensor method is proposed for the detection of faults in wind turbines from the SCADA data. The model sensor represents the dynamic relationship between the generator temperature, wind speed, and ambient temperature with the model structure derived from the first principles. When applied to SCADA data to conduct turbine fault detection, the parameters of the model sensor are updated every day by a parameter estimation process so that the model can timely represent the turbine operating conditions. Then, a NOFRFs based frequency analysis for the model sensor characteristics is carried out to extract damage sensitive indices and to perform fault detection based on the values of these indices. The new model sensor method is applied to 5 years' SCADA data of three operating wind turbines in Spain. The same data are also used for the traditional power curve and generator temperature analysis. The results show that the new method can not only correctly detect a generator fault with one of the three turbines but also reveal the trend of ageing with the turbine's winding

insulation so as to realise failure prognosis, which cannot be achieved by the traditional methods. The key idea with the proposed method is to use the changes in the properties of inspected systems to conduct system fault detection. The field data analysis in the present study has demonstrated the effectiveness of this novel idea and its potential applications in wind energy industry.

References

Aglen, O., 2003. Loss calculation and thermal analysis of a high-speed generator, in: Electric Machines and Drives Conference, IEEE, Madison. pp. 1117–1123.

Alvarez, E.J., Ribaric, A.P., 2018. An improved-accuracy method for fatigue load analysis of wind turbine gearbox based on scada. Renewable Energy 115, 391–399.

Barahona, B., Hoelzl, C., Chatzi, E., 2017. Applying design knowledge and machine learning to scada data for classification of wind turbine operating regimes, in: 2017 IEEE Symposium Series on Computational Intelligence, IEEE, Honolulu, HI, USA. pp. 1–8.

Carrillo, C., Montaño, A.O., Cidrás, J., Díaz-Dorado, E., 2013. Review of power curve modelling for wind turbines. Renewable and Sustainable Energy Reviews 21, 572–581.

Esfandiari, R.S., Lu, B., 2014. Modeling and analysis of dynamic systems. CRC Press, Boca Raton.

Feng, Y., Qiu, Y., Crabtree, C.J., Long, H., Tavner, P.J., 2011. Use of scada and cms signals for failure detection and diagnosis of a wind turbine gearbox, in: European Wind Energy Conference and Exhibition 2011, EWEC 2011, Sheffield. pp. 17–19.

Frank, P.M., 1990. Fault diagnosis in dynamic systems using analytical and knowledge-based redundancy: A survey and some new results. automatica 26, 459–474.

Ge, Z., Song, Z., 2010. A comparative study of just-in-time-learning based methods for online soft sensor modeling. Chemometrics and Intelligent Laboratory Systems 104, 306–317.

Gill, S., Stephen, B., Galloway, S., 2012. Wind turbine condition assessment through power curve copula modeling. IEEE Transactions on Sustainable Energy 3, 94–101.

Gray, C.S., Watson, S.J., 2010. Physics of failure approach to wind turbine condition based maintenance. Wind Energy 13, 395–405.

Hu, R.L., Leahy, K., Konstantakopoulos, I.C., Auslander, D.M., Spanos, C.J., Agogino, A.M., 2016. Using domain knowledge features for wind turbine diagnostics, in: 2016 15th IEEE International Conference on Machine Learning and Applications (ICMLA), IEEE. pp. 300–307.

Jia, X., Jin, C., Buzza, M., Wang, W., Lee, J., 2016. Wind turbine performance degradation assessment based on a novel similarity metric for machine performance curves. Renewable Energy 99, 1191–1201.

Kadlec, P., Gabrys, B., 2011. Local learning-based adaptive soft sensor for catalyst activation prediction. AIChE Journal 57, 1288–1301.

Kadlec, P., Gabrys, B., Strandt, S., 2009. Data-driven soft sensors in the process industry. Computers and Chemical Engineering 33, 795–814.

Lang, Z., Billings, S., 2005. Energy transfer properties of non-linear systems in the frequency domain. International Journal of Control 78, 345–362.

Leahy, K., Hu, R.L., Konstantakopoulos, I.C., Spanos, C.J., Agogino, A.M., 2016. Diagnosing wind turbine faults using machine learning techniques applied to operational data, in: 2016 IEEE International Conference on Prognostics and Health Management (ICPHM), IEEE. pp. 1–8.

Long, H., Wang, L., Zhang, Z., Song, Z., Xu, J., 2015. Data-driven wind turbine power generation performance monitoring. IEEE Transactions on Industrial Electronics 62, 6627–6635.

Lu, B., Li, Y., Wu, X., Yang, Z., 2009. A review of recent advances in wind turbine condition monitoring and fault diagnosis, in: Power Electronics and Machines in Wind Applications, IEEE, Lincoln, NE, USA. pp. 1–7.

Lydia, M., Kumar, S.S., Selvakumar, A.I., Kumar, G.E.P., 2014. A comprehensive review on wind turbine power curve modeling techniques. Renewable and Sustainable Energy Reviews 30, 452–460.

Pandit, R.K., Infield, D., 2018. Scada-based wind turbine anomaly detection using gaussian process models for wind turbine condition monitoring purposes. IET Renewable Power Generation 12, 1249–1255.

Pashazadeh, V., Salmasi, F.R., Araabi, B.N., 2018. Data driven sensor and actuator fault detection and isolation in wind turbine using classifier fusion. Renewable Energy 116, 99–106.

Peng, Z., Lang, Z., Billings, S., 2007. Crack detection using nonlinear output frequency response functions. Journal of Sound and Vibration 301, 777–788.

Peng, Z., Lang, Z., Wolters, C., Billings, S., Worden, K., 2011. Feasibility study of structural damage detection using narmax modelling and nonlinear output frequency response function based analysis. Mechanical Systems and Signal Processing 25, 1045–1061.

Qiu, Y., Feng, Y., Sun, J., Zhang, W., Infield, D., 2016. Applying thermophysics for wind turbine drivetrain fault diagnosis using scada data. IET Renewable Power Generation 10, 661–668.

Qiu, Y., Feng, Y., Tavner, P., Richardson, P., Erdos, G., Chen, B., 2012. Wind turbine scada alarm analysis for improving reliability. Wind Energy 15, 951–966.

Schlechtingen, M., Santos, I.F., 2014. Wind turbine condition monitoring based on scada data using normal behavior models. part 2: Application examples. Applied Soft Computing 14, 447–460.

Schlechtingen, M., Santos, I.F., Achiche, S., 2013. Wind turbine condition monitoring based on scada data using normal behavior models. part 1: System description. Applied Soft Computing 13, 259–270.

Shang, C., Yang, F., Huang, D., Lyu, W., 2014. Data-driven soft sensor development based on deep learning technique. Journal of Process Control 24, 223–233.

Shin, D., Chung, S.W., Chung, E.Y., Chang, N., 2010. Energy-optimal dynamic thermal management: computation and cooling power co-optimization. IEEE Transactions on Industrial Informatics 6, 340–351.

Shokrzadeh, S., Jozani, M.J., Bibeau, E., 2014. Wind turbine power curve modeling using advanced parametric and nonparametric methods. IEEE Transactions on Sustainable Energy 5, 1262–1269.

Söderström, T., Stoica, P., 1989. System identification. Prentice Hall.

Sun, P., Li, J., Wang, C., Lei, X., 2016. A generalized model for wind turbine anomaly identification based on scada data. Applied Energy 168, 550–567.

Tamura, J., 2012. Calculation method of losses and efficiency of wind generators, in: Wind Energy Conversion Systems. Springer, pp. 25–51.

Uluyol, O., Parthasarathy, G., Foslien, W., Kim, K., 2011. Power curve analytic for wind turbine performance monitoring and prognostics, in: Annual Conference of the Prognostics and Health Management Society, Montreal, Canada. pp. 1–8.

Wang, L., Zhang, Z., Long, H., Xu, J., Liu, R., 2017. Wind turbine gearbox failure identification with deep neural networks. IEEE Transactions on Industrial Informatics 13, 1360–1368.

Wilkinson, M., Darnell, B., Van Delft, T., Harman, K., 2014. Comparison of methods for wind turbine condition monitoring with scada data. IET Renewable Power Generation 8, 390–397.

Worden, K., Barthorpe, R., Cross, E., Dervilis, N., Holmes, G., Manson, G., Rogers, T., 2018. On evolutionary system identification with applications to nonlinear benchmarks. Mechanical Systems and Signal Processing 112, 194–232.

Yang, W., Court, R., Jiang, J., 2013. Wind turbine condition monitoring by the approach of scada data analysis. Renewable Energy 53, 365–376.

Zhang, F., Wen, Z., Liu, D., Jiao, J., Wan, H., Zeng, B., 2020. Calculation and analysis of wind turbine health monitoring indicators based on the relationships with scada data. Applied Sciences 10, 410.